ISSN: 0975-833X

Available online at http://www.journalcra.com

International Journal of Current Research
Vol. 10, Issue, 11, pp.75461-75467, November, 2018
DOI: https://doi.org/10.24941/ijcr.33200.11.2018

INTERNATIONAL JOURNAL OF CURRENT RESEARCH

RESEARCH ARTICLE

HUMAN CORNEAL STATE PREDICTION FROM TOPOGRAPHICAL MAPS USING A DEEP NEURAL NETWORK AND A SUPPORT VECTOR MACHINE

[1]Nazar Salih and [2]Nebras Hussein

[1]Master student: Electrical, Electronic, and Computer Engineering Department, Graduate School of Natural and Applied Science, Aksaray University, Aksaray, Turkey
[2]Assist. Prof., Biomedical Engineering Department, Al-Khawarizmi College of Engineering, Baghdad University, Baghdad, Iraq

ARTICLE INFO

Article History:
Received 10th August, 2018
Received in revised form
27th September, 2018
Accepted 19th October, 2018
Published online 30th November, 2018

Key Words:
Convolutional neural networks,
Deep learning, SVM,
Topographic images,
VGGNet-16

ABSTRACT

Precise diagnosis for a wide range of diseases infecting the human eye is a commitment. Therefore, developing new, smart algorithms is necessary to enhance doctors' diagnostic decisions. The recently invented Pentacam® is a measurement system that introduces topographic maps for the cornea, measures changes upon it, and helps doctors to make a precise diagnosis. This study extracts features from corneal topographic maps to improve the Pentacam® readings and further support precise diagnosing by using deep learning techniques, with an analytical view of the extracted features. A 16-layer convolutional neural network (CNN) was trained using the VGG-16 network to extract powerful features from corneal topographic maps. A sample of 732 human eyes were selected from enlarged topographic images from both genders (414 females and 318 males), divided into two groups: normal and abnormal. The patients' ages ranged from 12 to 76 years. The procedure of the study consisted of three major steps: (1) classification of the extracted features according to the refractive map type (where the estimated accuracy was 96.6%); (2) prediction of the clinical state (normal or abnormal) per individual map (where the estimated accuracy was 88.8%, 98.9%, 94.8%, and 94.5% for the sagittal map, the elevation front map, the elevation back map, and the corneal thickness map, respectively); and (3) comparison of the predicted results and clinical decision-making. The agreement between them reaches about 94.72%, which indicated the power and usefulness of the proposed algorithm.

***Citation: Nazar Salih and Nebras Hussein*, 2018.** "Human corneal state prediction from topographical maps using a deep neural network and a support vector machine", *International Journal of Current Research*, 10, (11), 75461-75467.

INTRODUCTION

The cornea is the outlying part of the human eye, of a domed shape, and transparent in nature (Camarillo *et al.,* 2002). It holds significant focusing power, and, as indicated by the World Health Organization (WHO), corneal blindness is one of the significant factors of visual deficiency and the fourth reason for corneal darkness all around (5.1%). Frequently, reports are incomplete, but 1.5 to 2.0 million new instances of unilateral darkness are rated annually (World Health Organization, n.d.). The Pentacam® is a powerful scanner for segments of the eye, based on the Scheimpflug camera measurements. It is a robust invention that helps ophthalmologists in investigating the corneal anterior surface (Smolek & Klyce, 1997)(Mazen M Sinjab, 2015). The four refractive maps in Figure 1 help to detect corneal disease (the sagittal map, the pachymetric or corneal thickness map, the elevation front map, and the elevation back map).

***Corresponding author:* Nazar Salih**,
Master student: Electrical, Electronic, and Computer engineering Department, Graduate School of Natural and Applied Science, Aksaray University, Aksaray, Turkey

Each map gives an indication about the eye, and after reviewing all of the features from the four refractive maps, a diagnostic decision can be made (Ali, Ghaeb, & Musa, n.d.). This paper presents a diagnostic method that uses deep learning to extract features from the four refractive maps provided by the Pentacam®, and then enters these features into the support vector machine (SVM) classifier for accurate diagnosing that supports the clinician's opinion. In this study, each normal indication will be written as NORMAL, and ABNORMAL will be written for the abnormal indications.

Deep Learning

Today, the classification of images is accomplished using deep learning techniques (Tan, Rajendra Acharya, Bhandary, Chua Chua, & Sivaprasad, n.d.). It combines both classification and feature extraction. These techniques can deliver great outcomes utilizing complicated networks built with large-scale data. For this study, we trained a Convolutional Neural Network (CNN) using deep learning to recognize and classify each of these topographic maps as normal or abnormal.

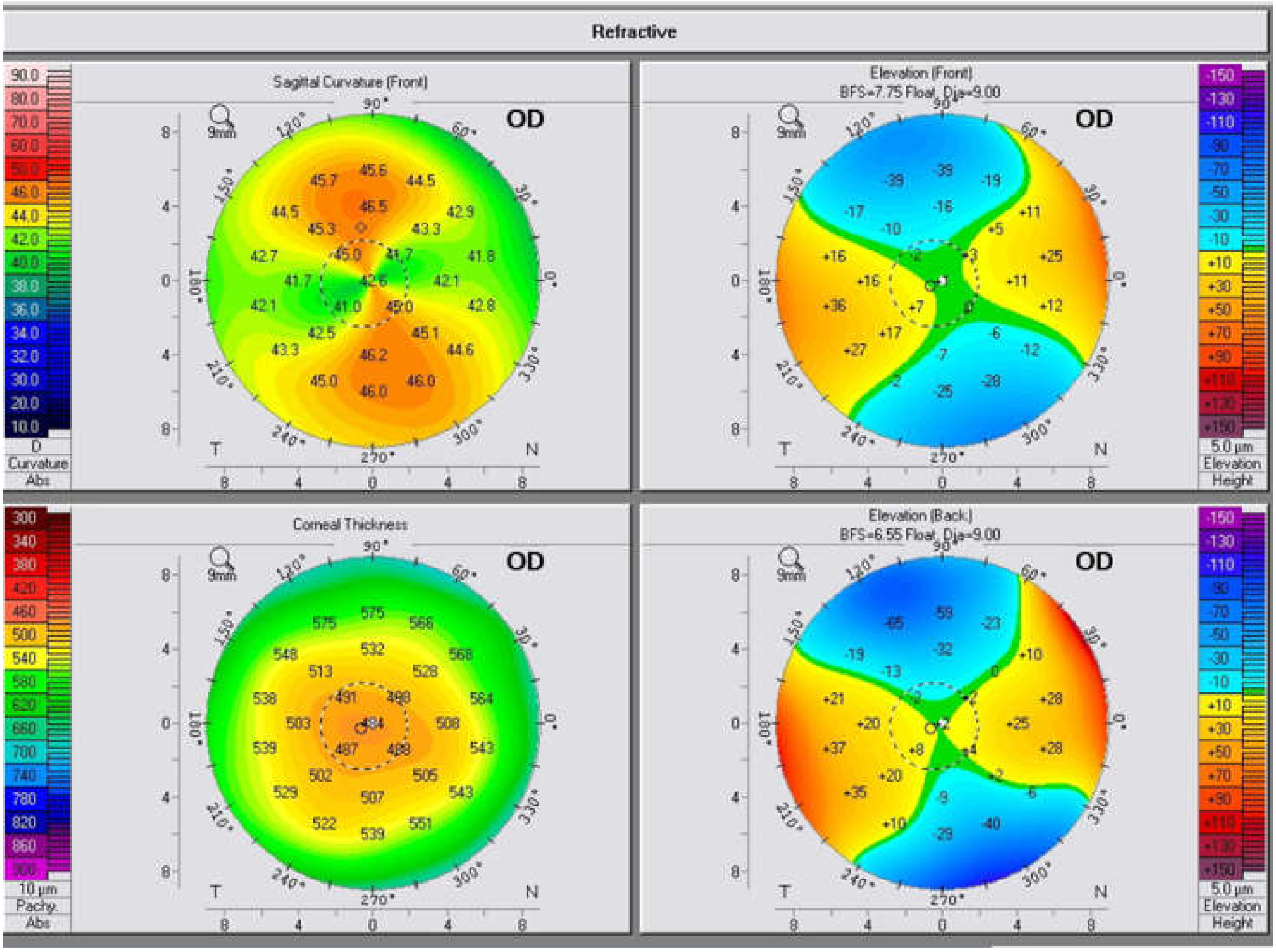

Fig. 1. Example of four refractive maps for corneal topography from the Pentacam®

During training, the features were extracted from the input images to provide a powerful and deep CNN model (the VGG-16 network was used here), and unknown images were classified efficiently during the testing stage. The particular structure of the trained network is explained below.

Convolutional Neural Network (CNN): In neural networks, CNN's are a deep learning model that contain multiple network layers. The more profound the network, the better it learns. It can self-learn furthermore self-organize without administration (Acharya *et al.,* 2018). The majority of the convolutional models will consist of the following operations, which can be considered as the building blocks of CNN's.

Image Input Layer: This layer should be available on all networks. This layer carries the input to the network and can utilize 2-D and 3-D images. The image dimension must be introduced here (Riesenhuber & Poggio, 1999).

Convolutional Layer: A convolutional layer is the most essential element of a CNN it implements a convolution task on the previous layer. A window is moved over the input image with a stride that is indicated by the client. In the wake of performing convolution, feature maps are generated and used as input for the next layer (Cireşan, Meier, & Schmidhuber, 2011) (Scherer, Müller, & Behnke, 2010).

Rectified Linear Unit (ReLU): The ReLU is one of the CNN layers in which, for each input element, a thresholding operation is performed. The decreases data repetition and maintains the significant features intact. The size of this layer's output is similar to the past layer (Raghavendra *et al.,* 2018).

Max Pooling Layer: Pooling layer is implemented to every map feature to diminish its size. The value of stride is typically chosen by the client. The extreme value over the window is considered and the window is supplanted by that number. The size of this layer's output is lower than that of the past layer (Cireşan *et al.,* 2011) (Scherer *et al.,* 2010)(Raghavendra *et al.,* 2018).

Fully Connected Layer (FC): The neurons will be selected from the previous layer and correlated to all neurons in this layer. The yield of FC will be the number of classifications (Serre, Wolf, & Poggio, 2005).

VGG-16 Network: The Visual Geometry Group (VGG) in conjunction with the University of Oxford's Department of Engineering Science, built up this design with 16 layers (Thoma, 2017)(Grassmann *et al.,* 2018). The VGG architecture has been one of the most popular CNN models since its introduction in 2014. The reason for its popularity is in its model simplicity and the use of small-sized convolutional kernels, which leads to very deep networks (Khan, Rahmani, Shah, & Bennamoun, 2018). The VGG-16 architecture strictly uses 3×3 convolution kernels with intermediate max-pooling layers for feature extraction and a set of three fully connected layers toward the end for classification. Each convolution layer is followed by a ReLU layer in the VGG architecture (Khan *et al.,* 2018). The motivation for selecting the VGG-16 network was its popularity and reputation for being user-friendly. The default data size for the VGG-16 model is 224×224 pixels ("Using Pre-Trained Models Keras," n.d.). The general design of the VGG-16 network can be found in Figure 2.

(268: 170 normal and 98 abnormal) and 20% for testing (67: 43 normal and 24 abnormal).

b. Elevation front map: 118 images were used; thus, it was applied to 80% of the sagittal images for training (94: 84 normal and 10 abnormal) and 20% for testing (23: 21 normal and 2 abnormal).

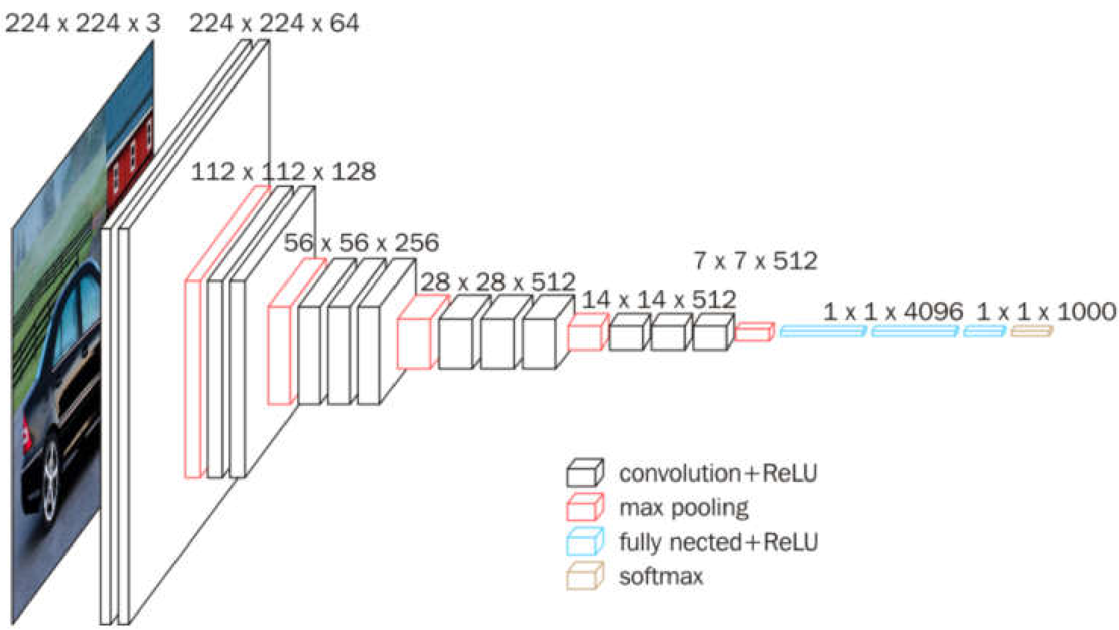

Fig. 2. VGG-16 Model Architecture (Abtosoftware, n.d.)

c. Elevation back map: 120 images were used; thus, it was applied to 80% of the sagittal images for training (96: 64 normal and 32 abnormal) and 20% for testing (24: 21 normal and 3 abnormal).
d. Corneal thickness map: 160 images were used; thus, it was applied to 80% of the sagittal images for training (128: 86 normal and 42 abnormal) and 20% for testing (32: 22 normal and 10 abnormal).

- Finally, collect the results for all refractive maps and determine whether the final result is normal or abnormal.

Support Vector Machine (SVM)

SVM which is a binary supervised classifier; it works by finding the maximum separating hyperplane between two classes of cases, for that SVM considered better in generalizing (Smitha, Shaji, & Mini, 2011). It maximizes the edges and for that creating the largest distance between the hyperplane separation and the cases on each side of it. It has been proven to reduce un upper limits on the generalization error expectations (Kotsiantis, Zaharakis, & Pintelas, 2006).

METHODOLOGY

Architecture: The VGG-16 network is a simpler model because of its limited use of hyperparameters. The network constantly uses 3×3 filters with a stride of 1 in the convolution layer and uses a similar padding in 2×2 pooling layers with a stride of 2. An overview of the VGG-16 network structure is seen above in Figure 2.

Training and Testing: The data is separated into training stage and testing stage. 80% of the chosen samples for training and 20% for testing. The features are extracted as follows:

- Determine the kind of refractive map (sagittal, corneal thickness, elevation front, or elevation back). In this study, 732 images were used; thus, 80% (586) of the images were used for training and 20% (146) for testing.
- Determine if these maps are normal or abnormal for each of the four refractive maps:
  a. Sagittal map: 334 images were used; thus, it was applied to 80% of the sagittal images for training

Data Analysis

Image dataset: The topographic maps for this work were collected from Al-Amal Eye Private Clinic, Baghdad, Iraq. The four refractive maps were gathered and transferred from the Pentacam® to a personal computer for analysis. The maps that were collected were of normal and abnormal corneas, as classified by the specialist. The sample four refractive maps are displayed in Figure 3.

RESULTS

The complete algorithm was worked in PYTHON 3.6.5 and achieved using a system configuration of Intel® Core™ i7-5500 CPU @ 2.40GHz, 16GB RAM. The first part of the evaluation was executed with images of size 224×224 with a learning rate of 1e-3. After dividing the dataset into training and testing sets, accuracy was computed for the evaluation. The greatest execution was achieved with a learning rate of 1e-3. By using an SVM classifier,a sample of 732 human eyes was selected from enlarged topographic images from both genders (414 females and 318 males), divided into two groups: normal and abnormal.

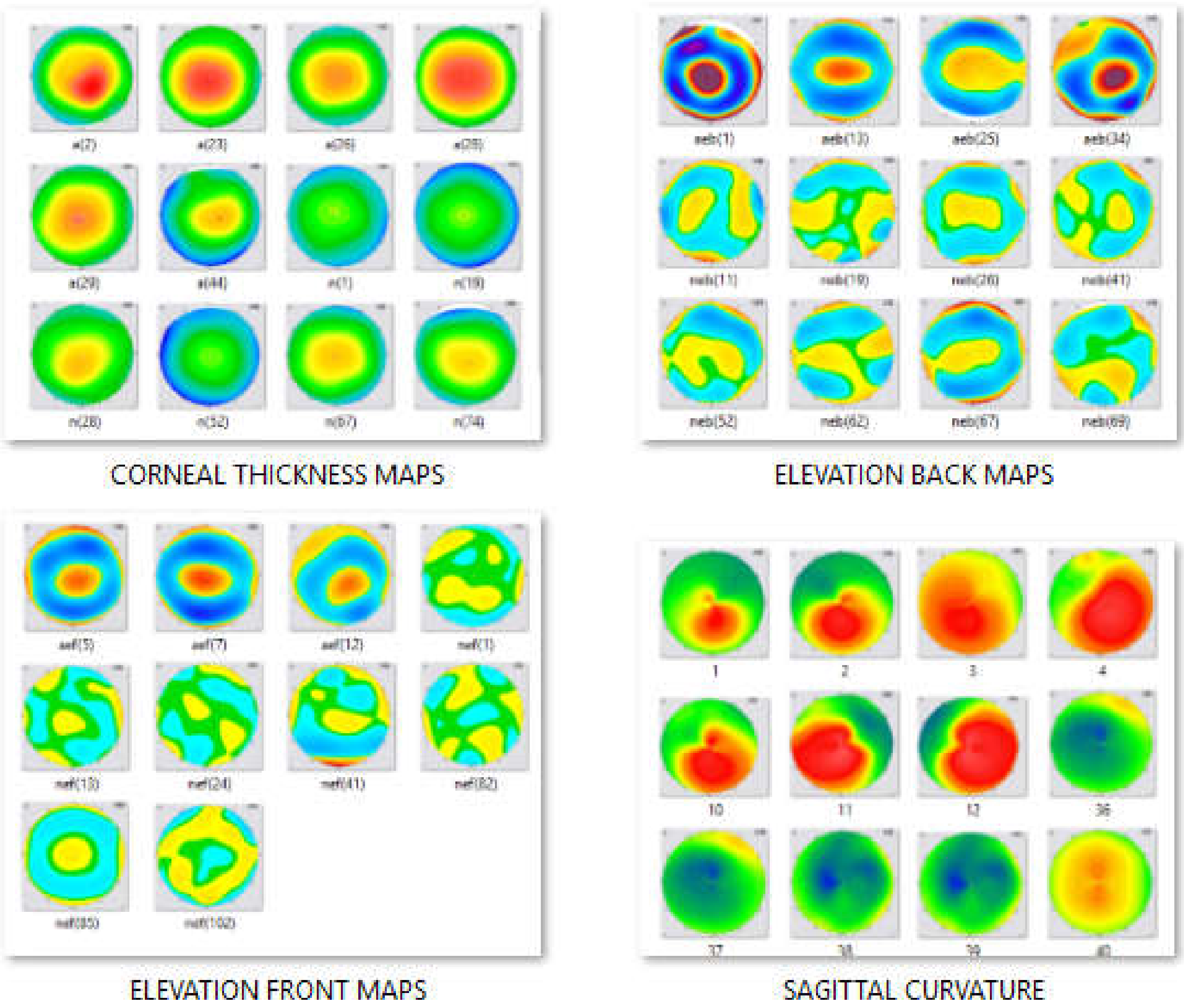

Fig. 3. Examples of corneal topographic maps

Table 1. The network's results

Validation results	
Model	Accuracy
type_of_map.model	96.6
sagittal_map.model	88.8
elevation_front_map.model	98.9
elevation_back_map.model	94.8
corneal_thickness_map.model	94.5

The age range of the patients was 12 to 76 years. The procedure of study consisted of three major steps: (1) classification of the extracted features according to the refractive map type (where the estimated accuracy was 96.6%); (2) prediction of the clinical state (normal or abnormal) per individual map (where the estimated accuracy was 88.8%, 98.9%, 94.8%, and 94.5% to sagittal map, elevation front map, elevation back map, and corneal thickness map, respectively) (see Table 1; and (3) the comparison of the predicted results and clinical decision-making. The agreement between them reaches about 94.72%, which indicated the power and usefulness of the proposed algorithm.

DISCUSSION

Commonly, a maximum number of images should be applied with using a CNN and VGG-16 network for real performance (Acharya *et al*., 2017), (Acharya *et al*., 2018). In this study, it was used on 732 topographic corneal images to extract features from them.

The network consists of 16 layers as shown in Figure 2. It was trained on the network for 100 epochs, achieving the extraction of features to train on a VGG-16 network on the corneal map dataset to distinguish between normal and abnormal maps. A model for each map was created separately:

- sagittal_map.model
- elevation_front_map.model
- elevation_back_map.model
- corneal_thickness_map.model

And it created a model for determining the type of map:

- type_of_map.model

The output of the training network for each model was as follows:

1. Sagittal map model

```
Epoch 95/100
8/8 [==============================] - 3s 413ms/step - loss: 0.2878 - acc: 0.8866
Epoch 96/100
8/8 [==============================] - 4s 456ms/step - loss: 0.3369 - acc: 0.8662
Epoch 97/100
8/8 [==============================] - 4s 496ms/step - loss: 0.2970 - acc: 0.8633
Epoch 98/100
8/8 [==============================] - 4s 455ms/step - loss: 0.2745 - acc: 0.9133
Epoch 99/100
8/8 [==============================] - 4s 452ms/step - loss: 0.3037 - acc: 0.8817
Epoch 100/100
8/8 [==============================] - 4s 450ms/step - loss: 0.3831 - acc: 0.8018
[INFO] serializing network...
[INFO] serializing label binarizer...
Training classifier and save
Finished training on data: dataset/data_maps/sagittal
```

Fig. 4. 80.18% classification accuracy on the training set (sagittal map)

2. Elevation front map model

```
Epoch 95/100
2/2 [==============================] - 1s 517ms/step - loss: 0.0141 - acc: 1.0000
Epoch 96/100
2/2 [==============================] - 1s 477ms/step - loss: 0.0722 - acc: 0.9688
Epoch 97/100
2/2 [==============================] - 1s 513ms/step - loss: 0.0778 - acc: 0.9688
Epoch 98/100
2/2 [==============================] - 1s 499ms/step - loss: 0.0223 - acc: 1.0000
Epoch 99/100
2/2 [==============================] - 1s 477ms/step - loss: 0.0579 - acc: 0.9531
Epoch 100/100
2/2 [==============================] - 1s 520ms/step - loss: 0.0277 - acc: 1.0000
[INFO] serializing network...
[INFO] serializing label binarizer...
Training classifier and save
Finished training on data: dataset/data_maps/elevation_front
```

Fig. 5. 100% classification accuracy on the training set (elevation front map)

3. Elevation back map model

```
Epoch 95/100
3/3 [==============================] - 2s 502ms/step - loss: 0.1848 - acc: 0.9167
Epoch 96/100
3/3 [==============================] - 1s 492ms/step - loss: 0.1688 - acc: 0.9375
Epoch 97/100
3/3 [==============================] - 1s 497ms/step - loss: 0.1382 - acc: 0.9688
Epoch 98/100
3/3 [==============================] - 2s 503ms/step - loss: 0.1563 - acc: 0.9583
Epoch 99/100
3/3 [==============================] - 2s 505ms/step - loss: 0.1303 - acc: 0.9688
Epoch 100/100
3/3 [==============================] - 1s 499ms/step - loss: 0.1368 - acc: 0.9375
[INFO] serializing network...
[INFO] serializing label binarizer...
Training classifier and save
Finished training on data: dataset/data_maps/elevation_back
```

Fig. 6. 93.75% classification accuracy on the training set (elevation back map)

4. Corneal thickness map model

```
Epoch 95/100
4/4 [==============================] - 2s 495ms/step - loss: 0.1261 - acc: 0.9609
Epoch 96/100
4/4 [==============================] - 2s 507ms/step - loss: 0.1225 - acc: 0.9688
Epoch 97/100
4/4 [==============================] - 2s 505ms/step - loss: 0.1320 - acc: 0.9688
Epoch 98/100
4/4 [==============================] - 2s 502ms/step - loss: 0.1273 - acc: 0.9531
Epoch 99/100
4/4 [==============================] - 2s 506ms/step - loss: 0.1275 - acc: 0.9531
Epoch 100/100
4/4 [==============================] - 2s 496ms/step - loss: 0.1321 - acc: 0.9375
[INFO] serializing network...
[INFO] serializing label binarizer...
Training classifier and save
Finished training on data: dataset/data_maps/corneal_thickness
```

Fig. 7. 93.75% classification accuracy on the trainingset (corneal thickness map)

5. Type of map model

```
Epoch 95/100
17/17 [==============================] - 8s 484ms/step - loss: 0.0880 - acc: 0.9717 - val_loss: 0.1035 - val_acc: 0.9333
Epoch 96/100
17/17 [==============================] - 8s 480ms/step - loss: 0.0998 - acc: 0.9632 - val_loss: 0.1340 - val_acc: 0.9000
Epoch 97/100
17/17 [==============================] - 8s 476ms/step - loss: 0.0829 - acc: 0.9687 - val_loss: 0.0461 - val_acc: 1.0000
Epoch 98/100
17/17 [==============================] - 8s 474ms/step - loss: 0.0927 - acc: 0.9698 - val_loss: 0.0630 - val_acc: 1.0000
Epoch 99/100
17/17 [==============================] - 8s 475ms/step - loss: 0.0635 - acc: 0.9871 - val_loss: 0.1260 - val_acc: 0.8667
Epoch 100/100
17/17 [==============================] - 8s 490ms/step - loss: 0.0777 - acc: 0.9651 - val_loss: 0.0374 - val_acc: 1.0000
```

Fig. 8. 100% classification accuracy on the training set (type of map)

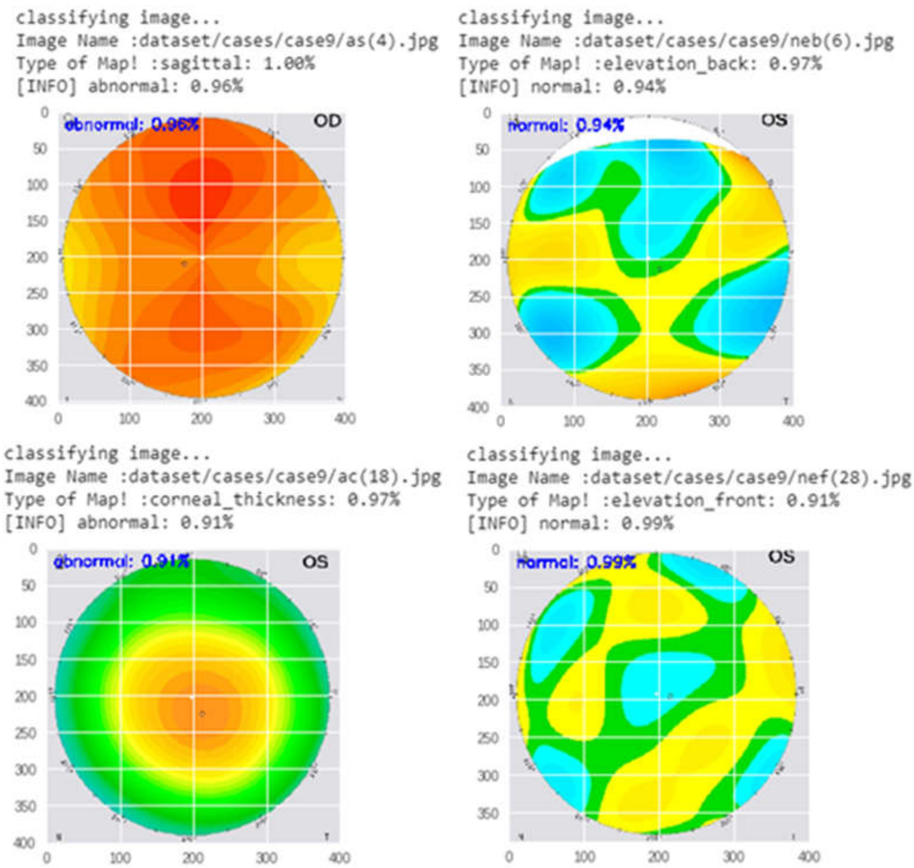

Fig. 9. Correctly classifying (normal and abnormal) images and kinds of map using the VGG-16 network

Conclusion

Corneal diseases are one of the leading problems of eye darkness, and a large percent of the worldwide population is influenced by it. The VGG-16 network obtained the highest accuracy of 96.6% in determining the type of maps. Also, it achieved 88.8%, 98.9%, 94.8%, and 94.5% accuracy in determining whether each was normal or abnormal (sagittal map, elevation front map, elevation back map, and corneal thickness map), respectively. The trained CNN model can expeditiously discover the class (normal or abnormal) and type of refractive maps of an unknown image (see Figure 9). Hence, ophthalmologists should focus their interest more on the normal cases to diminish their workload by about half. These models can help ophthalmologists to cross-check their clinical findings.

List of Abbreviations

AI Artificial Intelligence
ANNs Artificial Neural Networks
CNN Convolutional Neural Network
FC Fully Connected
GPU Graphics Processing Unit
GUI Graphical User Interface
SVM Support Vector Machine
VGG Visual Geometry Group
WHO World Health Organization

Acknowledgment

Special thanks goes to Al-Amal Eye Private Clinic in Baghdad, Iraq for permitting the use of their eye image database.

REFERENCES

Abtosoftware. (n.d.). Kitchen Furniture & Appliances Recognition - Abto Software, Lviv, Ukraine.

Acharya, U. R., Fujita, H., Lih, O. S., Adam, M., Tan, J. H., & Chua, C. K. 2017. Automated detection of coronary artery disease using different durations of ECG segments with convolutional neural network. Knowledge-Based Systems. https://doi.org/10.1016/j.knosys.2017.06.003

Acharya, U. R., Fujita, H., Oh, S. L., Raghavendra, U., Tan, J. H., Adam, M., … Hagiwara, Y. 2018. Automated identification of shockable and non-shockable life-threatening ventricular arrhythmias using convolutional neural network. Future Generation Computer Systems, 79, 952–959. https://doi.org/10.1016/J.FUTURE.2017.08.039

Ali, A. H., Ghaeb, N. H., & Musa, Z. M. (n.d.). Support Vector Machine for Keratoconus Detection by Using Topographic Maps with the Help of Image Processing Techniques. *IOSR Journal of Pharmacy and Biological Sciences* (IOSR-JPBS, 12(6), 50–58. https://doi.org/10.9790/3008-1206065058

Camarillo, T., Choi, K., Hamilton, G., Miles, M., Muller, K., Williams, K., … Schrepel, P. 2002. Athletes as an Ideal Target Population for Orthokeratology Keratoconus : Improving Quality of Life Through Advancements in Detection and Treatment.

Cireşan, D., Meier, U., & Schmidhuber, J. 2011. A committee of neural networks for traffic sign classification. In Proceedings of the International Joint Conference on Neural Networks. https://doi.org/ 10.1109/ IJCNN.2011.6033458

Grassmann, F., Mengelkamp, J., Brandl, C., Harsch, S., Zimmermann, M. E., Linkohr, B., … Weber, B. H. F. 2018. A deep learning algorithm for prediction of age-related eye disease study severity scale for age-related macular degeneration from color fundus photography. Ophthalmology, 125(9), 1410–1420. https://doi.org/ 10.1016/j.ophtha.2018.02.037

Khan, S., Rahmani, H., Shah, S. A. A., & Bennamoun, M. 2018. A Guide to Convolutional Neural Networks for Computer Vision. Synthesis Lectures on Computer Vision (Vol. 8). https://doi.org/10.2200/ S00822 ED1V01Y201712COV015

Kotsiantis, S. B., Zaharakis, I. D., & Pintelas, P. E. 2006. Machine learning: A review of classification and combining techniques. *Artificial Intelligence Review*, 26(3), 159–190. https://doi.org/10.1007/s10462-007-9052-3

Mazen M Sinjab. 2015. Step by Step Reading Pentacam Topography (Basics and Case Study Series).

Raghavendra, U., Fujita, H., Bhandary, S. V., Gudigar, A., Tan, J. H., & Acharya, U. R. 2018. Deep convolution neural network for accurate diagnosis of glaucoma using digital fundus images. Information Sciences, 441, 41–49. https://doi.org/10.1016/j.ins.2018.01.051

Riesenhuber, M., & Poggio, T. 1999. Hierarchical models of object recognition in cortex. Nature Neuroscience, 2(11), 1019–1025. https://doi.org/10.1038/14819

Scherer, D., Müller, A., & Behnke, S. 2010. Evaluation of pooling operations in convolutional architectures for object recognition. In Lecture Notes in Computer Science (including subseries Lecture Notes in Artificial Intelligence and Lecture Notes in Bioinformatics). https://doi.org/ 10.1007/978-3-642-15825-4_10

Serre, T., Wolf, L., & Poggio, T. 2005. Object recognition with features inspired by visual cortex. In Proceedings - 2005 IEEE Computer Society Conference on Computer Vision and Pattern Recognition, CVPR 2005. https://doi.org/ 10.1109/CVPR.2005.254

Smitha, P., Shaji, L., & Mini, M. G. 2011. A Review of Medical Image Classification Techniques. International Conference on VLSI, Communication & Instrumentation, (Icvci), 34–38.

Smolek, M. K., & Klyce, S. D. 1997. Current keratoconus detection methods compared with a neural network approach. *Invest Ophthalmol.Vis.Sci.,* 38(0146–0404 (Print)), 2290–2299.

Tan, J. H., Rajendra Acharya, U., Bhandary, S. V, Chua Chua, K., & Sivaprasad, S. (n.d.). Segmentation of optic disc, fovea and retinal vasculature using a single convolutional neural network.

Thoma, M. 2017. Analysis and Optimization of Convolutional Neural Network Architectures. CoRR.

Using Pre-Trained Models Keras. (n.d.).

World Health Organization. (n.d.). Priority Eye Diseases.

****